Molten Salt Vapour Corrosion of Ti_3Al and TiAl Based Intermetallics

Kai Zhang, Zhengwei Li, Michael A. Hodgson and Wei Gao*

Department of Chemical and Materials Engineering
The University of Auckland, New Zealand

(Received July 2, 2002)

ABSTRACT

Hot corrosion tests were performed with Ti_3Al, Ti-44Al, Ti-48Al, Ti-52Al, Ti-48Al-2Cr and Ti_3Al-11Nb (at%) intermetallics. The salt mixture used in the present study consisted of 80wt%Na_2SO_4 + 20wt%NaCl, with a melting point of ~700°C. The specimens were suspended in the salt vapour at 800°C. It was found that the hot corrosion resistance generally increases with increasing Al content. Ti-48Al-2Cr showed the best corrosion resistance due to its relatively high Al content and Cr addition. Ti_3Al-11Nb unexpectedly showed poor corrosion resistance. It is suggested that the Nb addition might accelerate the formation of sulphide at the interface, playing a detrimental role in the corrosion process. Electron microscopy and X-ray diffraction were used to study the morphologies, compositions, and phases of the corrosion products. The mechanisms of hot corrosion were also discussed based on the experimental results.

Keywords:
Titanium aluminide; Molten salt corrosion; Corrosion and oxidation; Kinetics; Metals and alloys.

1. INTRODUCTION

Titanium, titanium alloys and titanium aluminide intermetallic compounds have been receiving considerable attention, as they are light weight and have excellent mechanical properties /1/. They also possess a number of excellent high temperature properties including creep resistance, fatigue resistance and static strength retention /2,3/. Therefore, they are being considered as the replacement of some Ni-based superalloys /4-7/. The main applications of titanium alloys have been in aerospace, chemical and petrochemical, metallurgical, papermaking, and medical industries. These applications require not only excellent mechanical properties, but also good high temperature resistance in corrosive environments /8/. However, the studies on titanium based materials have mainly been concentrated on the mechanical properties and oxidation behaviour in ambient air. Very little work has been carried out on the hot corrosion of these materials in salt-containing environments /9-13/.

The present work studies the hot corrosion behaviour of six titanium-aluminium based intermetallics in a mixed molten salt vapour

* Corresponding author:
Tel.: +64-9-3737599 ext. 8175; fax: +64-9-3737463;
E-mail address: w.gao@auckland.ac.nz

representing a fuel combustion and marine environment. The purpose of this paper is to investigate the general hot corrosion behaviour of Ti-Al intermetallics containing various amounts Al (30-52 at%), and with ternary alloying elements (Cr or Nb); and to discuss the effects of composition on the hot corrosion resistance.

2. EXPERIMENTAL PROCEDURE

2.1. Materials and specimen preparation

Six Ti-Al intermetallics were used in the present studies: Ti_3Al, Ti-44Al, Ti-48Al, Ti-52Al, Ti-48Al-2Cr and Ti_3Al-11Nb (compositions in at.%). Ti_3Al consists of a single α_2 phase, Ti-44Al consists of α_2 and γ phases, Ti-48Al consists mainly of γ-TiAl with a small amount of $\alpha_2(Ti_3Al)$; Ti-52Al consists of γ phase; and Ti-48Al-2Cr consists of near γ-phase.

The specimens, with dimensions of about 15×10×2 mm, were cut from the Ti-Al alloy ingots with a diamond saw. All the surfaces were ground to 600 grit finish, then ultrasonically degreased in ethanol, followed by blow drying. The mass of each specimen was measured using an electronic balance with an accuracy of 0.01 mg.

2.2. Hot corrosion testing method

Hot corrosion tests were carried out with 80 wt%Na_2SO_4 + 20 wt%NaCl salts as the corrosive agent at 800°C for 200 hr. The melting point of the mixed salts is about 700°C. Molten salt corrosion is a complex process that is influenced by experimental methods. Figure 1 shows the experimental setup /14/. The specimens were suspended with hooks in a covered crucible containing molten salts. The crucible with samples was then put into the hot zone of a furnace running at 800°C. The specimens did not contact the molten salt directly. The molten salt vaporised, therefore, the specimens were surrounded by the salt vapour. After a certain time of exposure, the specimens were withdrawn from the crucible, cooled in air, washed in boiling water to remove any salt left on the surface, cleaned with a soft brush, washed again, and dried in hot air. The masses of the specimen were then re-

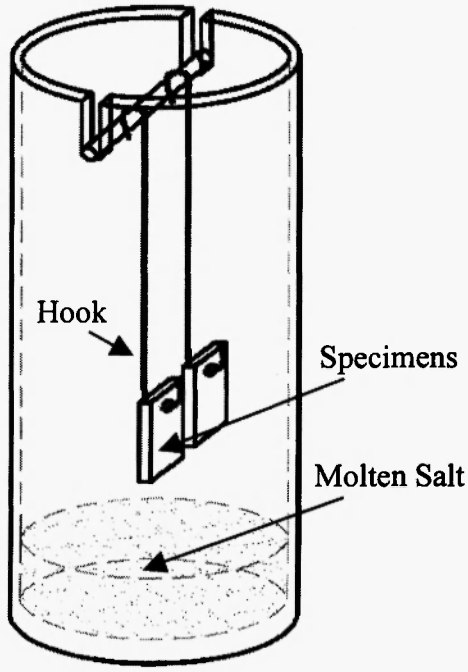

Fig. 1: Schematic of hot-corrosion test setup: specimens were suspended in salt vapour.

measured to obtain the mass changes for establishing the corrosion kinetics. The reaction kinetics measured by this method were relatively reproducible as the corrosion conditions were easy to control /15/.

2.3. Specimen characterization

The corroded specimens were analysed using an X-ray diffractometer (Bruker, D8) with a Cu-Kα radiation source, a scanning electron microscope (FEG-SEM, Philips XL 30S) with an energy dispersive X-ray analysis system (EDS).

3. RESULTS

Figure 2 represents the hot corrosion kinetics of all samples at 800°C in salt vapour. Curves could be classified into two groups according to their shapes and developing tendency. The first group includes Ti-48Al, Ti-52Al and Ti-48Al-2Cr (Fig. 2a); their mass gains were larger than the scale spallations. In the initial 20 hr exposure, these three specimens showed relatively small mass changes. After that, small scale spallation occurred on Ti-52Al and Ti-48Al-2Cr. Ti-48Al-2Cr had much

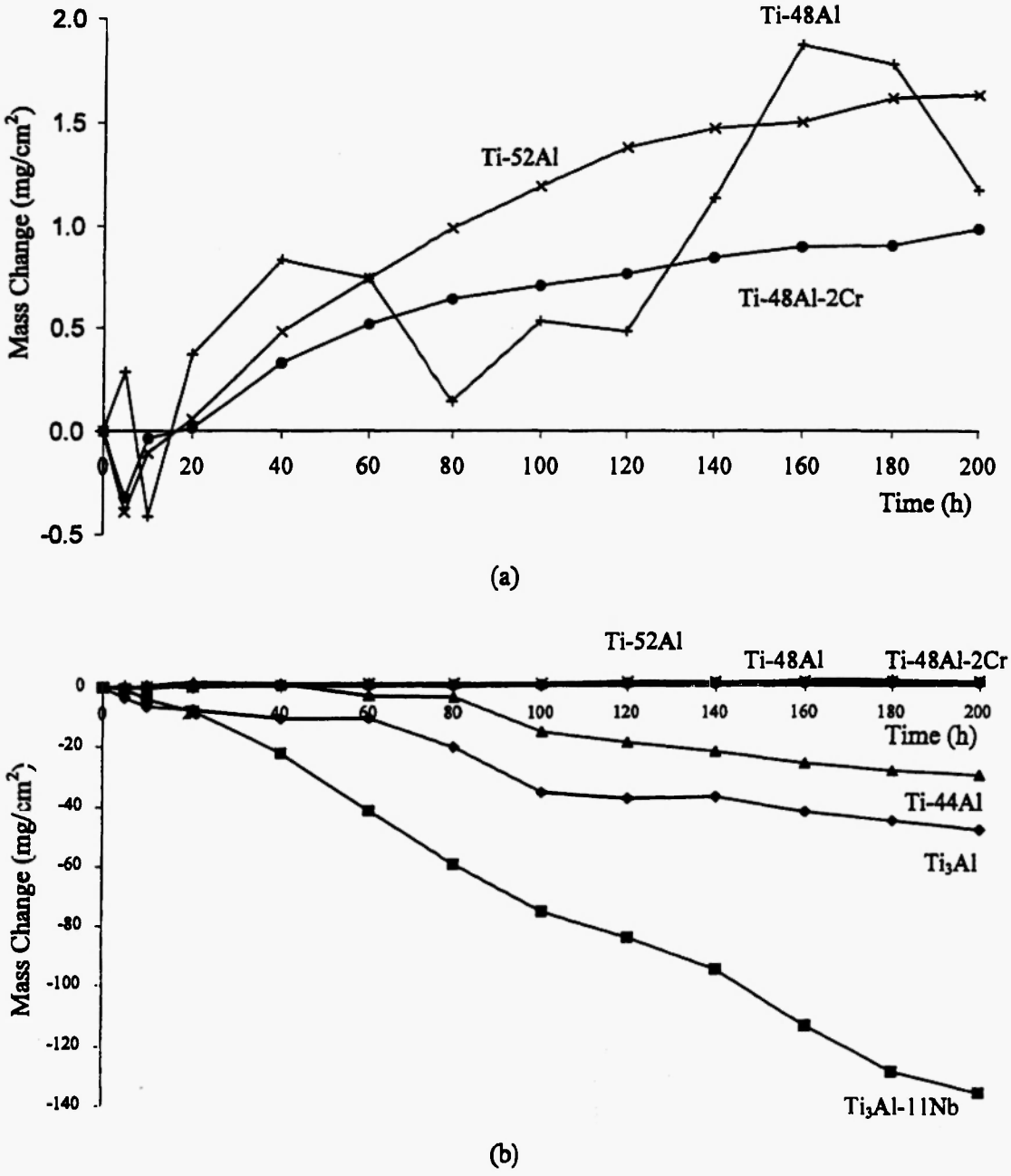

Fig. 2: Hot corrosion kinetics of specimens in Na_2SO_4 + 20 wt%NaCl salt vapour at 800°C.

lower mass gains, about half of Ti-52Al after 200 hr hot corrosion. The corrosion kinetics of Ti-52Al and Ti-48Al-2Cr followed an apparently parabolic rate law. However, the corrosion kinetics of Ti-48Al was not smooth, showing severe spallation during some cooling time periods. Scale spallation was observed on Ti-48Al, the oxide scale grew quickly, resulting in net mass gain up to 200 hr of exposure.

The second group of materials, Ti_3Al, Ti-44Al, Ti_3Al-11Nb, exhibited severe spallation after 200 hr hot corrosion test, especially for Ti_3Al-11Nb, with a mass loss about 135 mg/cm^2 (Fig. 2b). The scale spallation of these three specimens was easily observed with the naked eye at each cooling interval. Almost the whole thick oxide scale on Ti_3Al-11Nb spalled away at every cooling period. Generally, hot corrosion resistance of

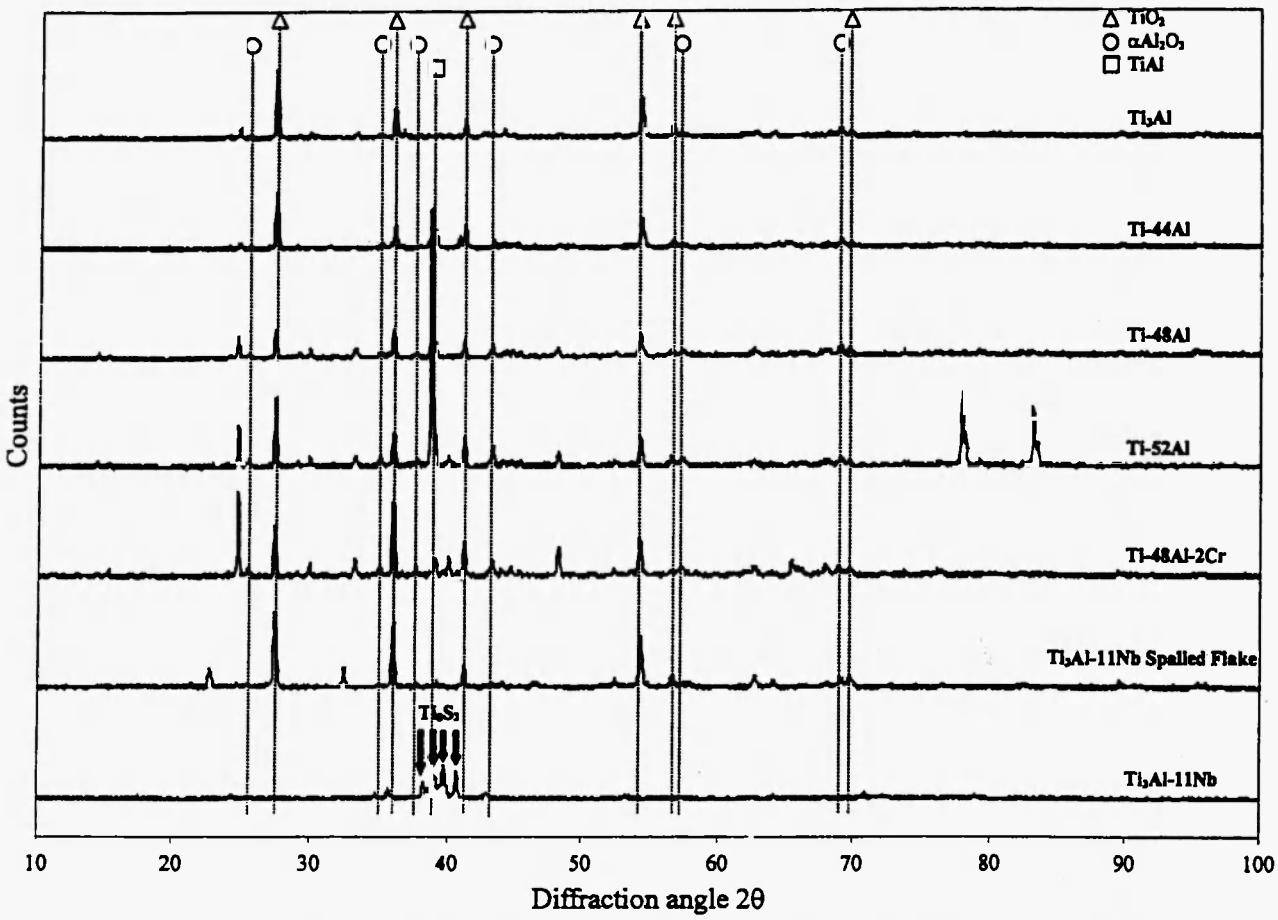

Fig. 3: X-ray diffraction spectra of the corrosion products formed on Ti-Al intermetallics after 200 hr exposure at 800°C.

these specimens could be put in the order (from the best) of Ti-48Al-2Cr, Ti-52Al, Ti-48Al, Ti-44Al, Ti_3Al and Ti_3Al-11Nb.

Figure 3 shows the XRD spectra of the corrosion products remaining on these specimens. The main corrosion products were TiO_2 and α-Al_2O_3, except Ti_3Al-11Nb. Most of the scale on the Ti_3Al-11Nb samples spalled away. The scale was collected and characterized with XRD. The results showed that they were mainly a mixture of TiO_2 and α-Al_2O_3. A small amount of Ti_8S_3 was detected on the surface of Ti_3Al-11Nb.

Figures 4-7 show the cross-section morphologies of the specimens after 200 hr hot corrosion at 800°C. It should be noted that these just show the scale that remained on the surface. From Fig. 4, it can be seen that the scale that remained on some parts of the Ti_3Al surface was still very thick. On some other locations, the substrate material was directly exposed to the corrosion environment. In Fig. 5, it can be seen that the mounting epoxy penetrated into the scale-alloy interface on the sample of Ti-48Al, providing evidence of severe cracking throughout the scale. For all specimens, the non-protective TiO_2 scale, even mixed with Al_2O_3, was easily broken. Figures 4 and 5 showed that the scale formed on Ti_3Al and Ti-48Al was porous and non-uniform, which was of non-protective nature, and were easy to break away from the substrate. When the scale spalled away, metal was directly exposed to the corrosive environments, resulting in an accelerated corrosion process. The poor corrosion resistance may be caused by two reasons. Firstly, Ti_3Al and Ti-48Al contains relatively low Al content. The activity of Al in Ti-Al systems decreases sharply around 50 at.%Al,

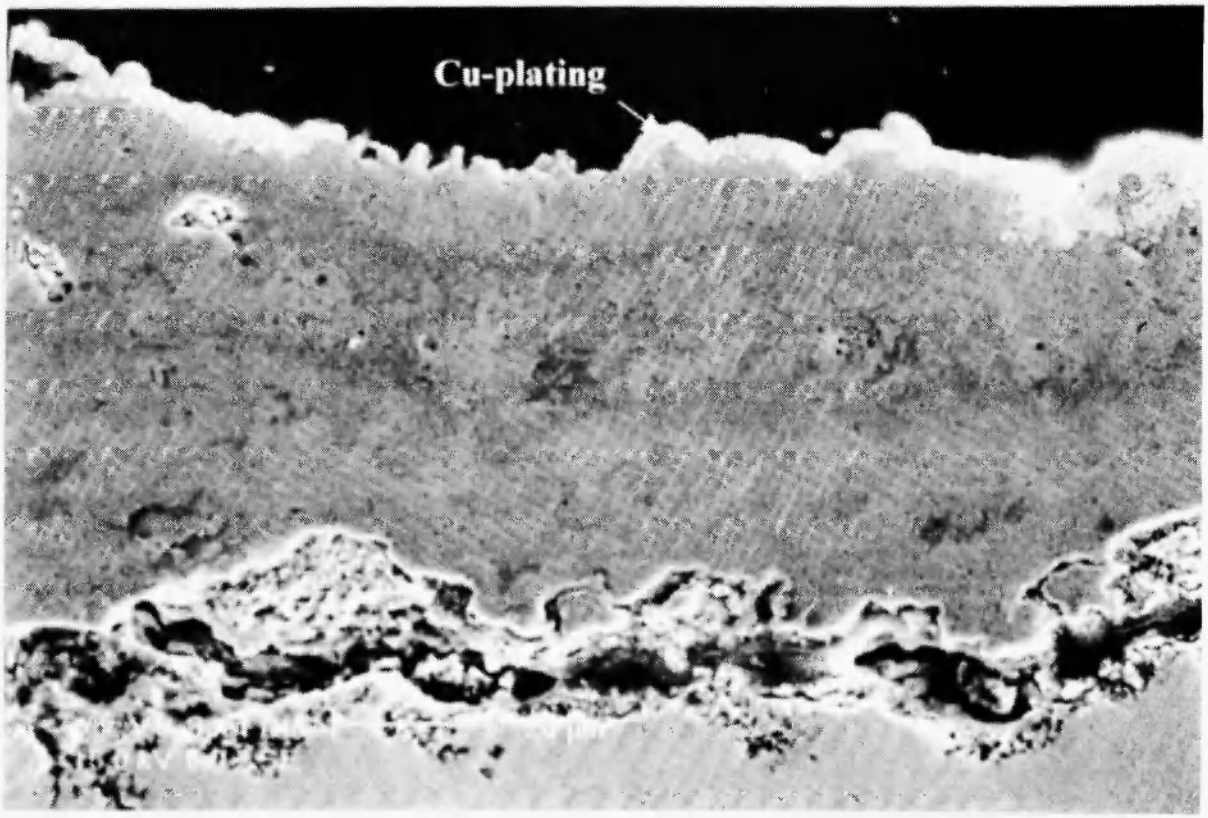

Fig. 4: Cross-section of Ti_3Al after 200 hr hot corrosion in Na_2SO_4 + 20 wt.%NaCl vapour at 800°C.

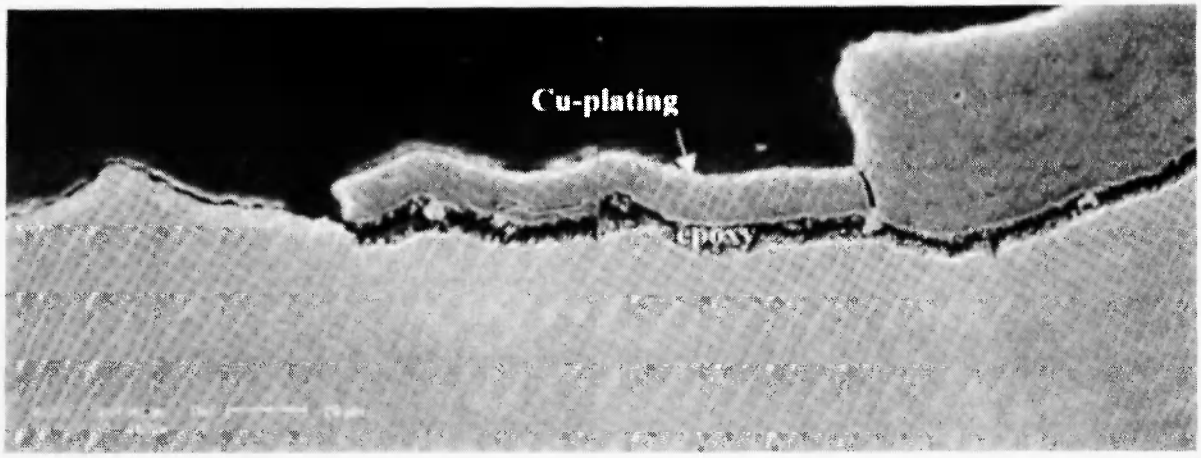

Fig. 5: Cross-section of Ti-48Al after 200 hr hot corrosion in Na_2SO_4 + 20 wt.%NaCl vapour at 800°C.

resulting in a higher oxidation rate of Ti. Secondly, as reported, Ti-48Al has a multi-phase structure, but Ti-52Al and Ti-48Al-2Cr consist of γ- or near γ-phase. The corrosion properties were often affected by the microstructure of the alloy. Figure 6 shows a thin, uniform and dense scale remaining on the Ti-48Al-2Cr surfaces. Figure 7 shows the cross-section of Ti_3Al-11Nb after 200 hr exposure. The light section (marked

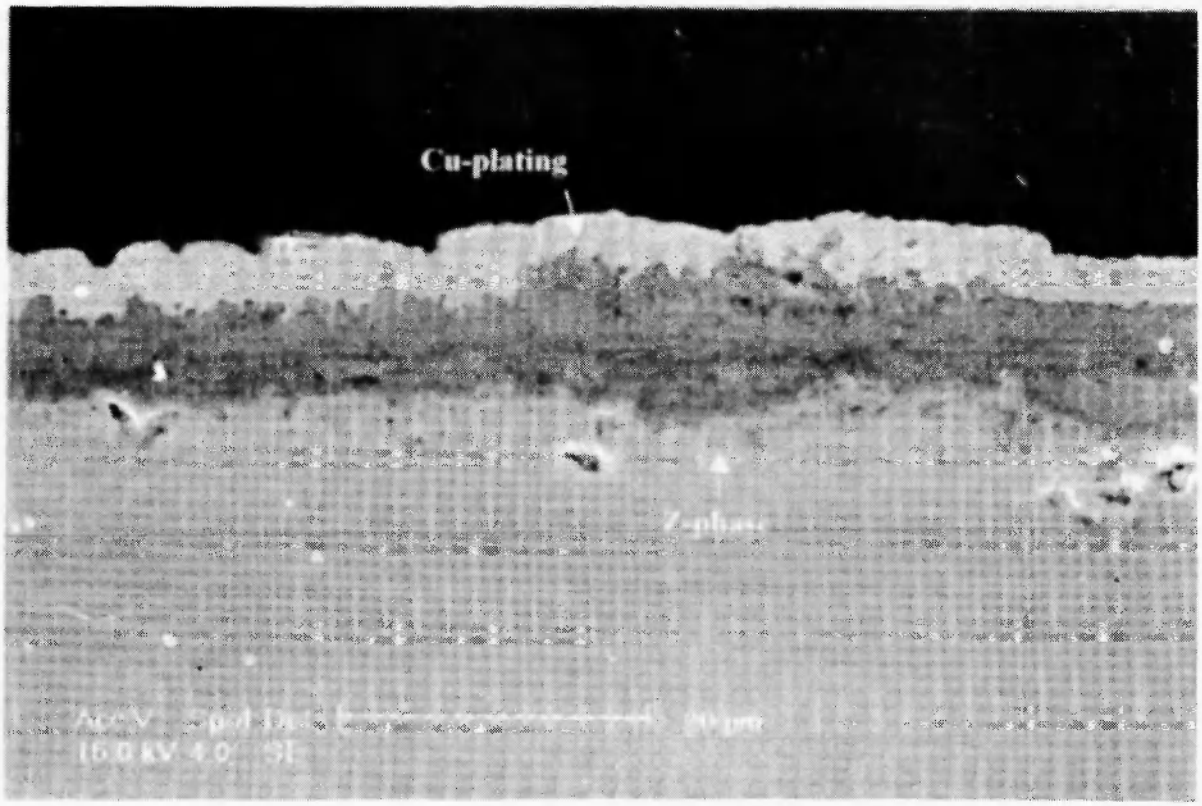

Fig. 6: Cross-section of Ti-48Al-2Cr after 200 hr hot corrosion in Na_2SO_4 + 20 wt.%NaCl vapour at 800°C.

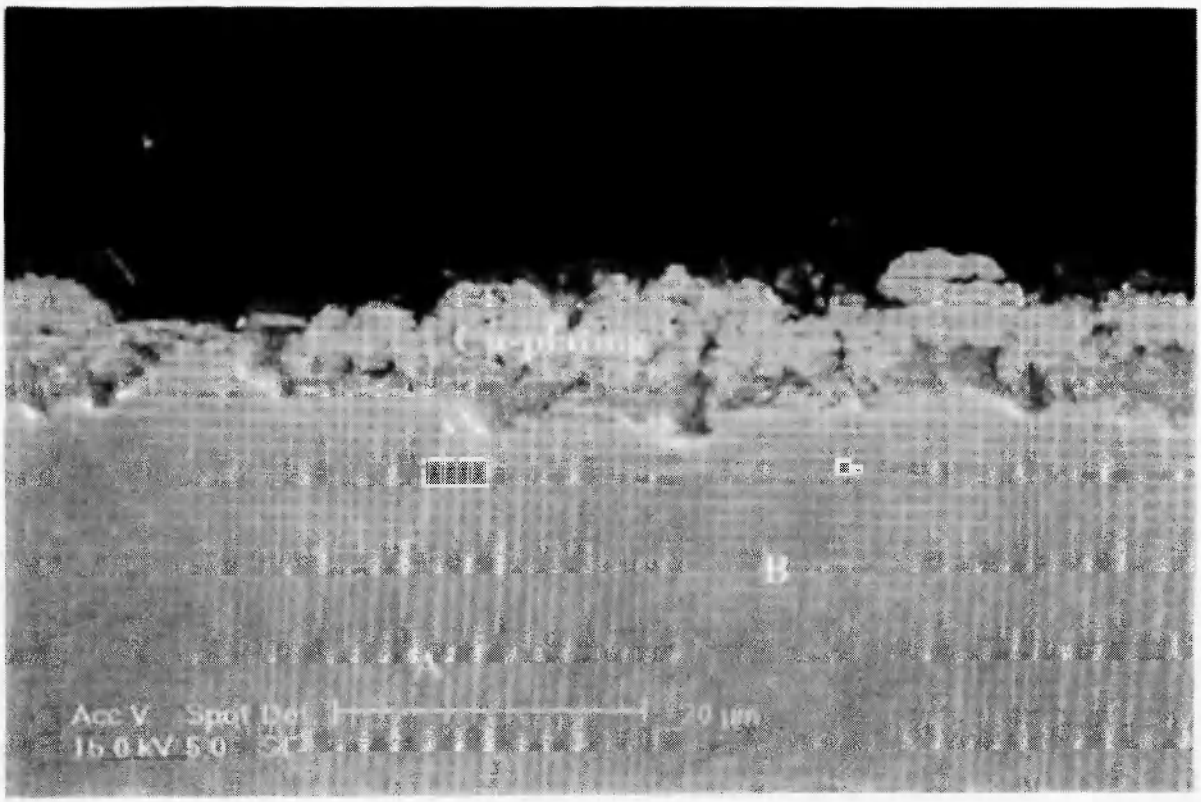

Fig. 7: Cross-section of Ti_3Al-11Nb after 200 hr hot corrosion in Na_2SO_4 + 20 wt.%NaCl vapour at 800°C.

A) has a composition of Al = 23.59, Ti = 64.84, Nb = 11.57, while the dark section (marked B) has Al = 23.83, Ti = 65.50, Nb = 10.66, in at. %. This implies that the A section is slightly enriched in Nb, but the concentration difference was not great. This difference might be due to diffusion of Nb during the heat treatment. From Fig. 7, little scale could be found on the surface. The Ti_8S_3 phase detected on the scale formed on Ti_3Al-11Nb by XRD might be very thin or distributed non-uniformly.

4. DISCUSSION

The corrosion kinetics of Ti_3Al-11Nb, Ti_3Al and Ti-44Al followed an apparently linear rate law, resulting in large mass losses. The corrosion kinetics of Ti-48Al was not smooth, and this specimen showed severe spallation during some cooling stages. Ti-52Al and Ti-48Al-2Cr showed the best corrosion resistance among these six Ti-Al based intermetallics.

The reactions in hot corrosion often have complex mechanisms. Simplified processes, however, could be suggested as below. Al_2O_3 and TiO_2 were formed on the alloy surface at the beginning in an O_2-containing environment. With salt vapour in the atmosphere, it was possible that TiO_2 and Al_2O_3 reacted with NaCl /16/.

$$2NaCl + Al_2O_3 + 1/2O_2 \rightarrow 2NaAlO_2 + Cl_2 \quad (1)$$

$$NaCl + TiO_2 + O_2 \rightarrow NaTiO_4 + 1/2Cl_2 \quad (2)$$

Penetration and transportation of Cl_2 (Cl^-, Cl), and reaction of Cl species with Al and /or Ti in the substrate surface might follow:

$$Ti + Cl_2 \rightarrow TiCl_2 \quad (3)$$

$$Al + 3/2Cl_2 \rightarrow AlCl_3 \quad (4)$$

On the surface of the scale, where the oxygen potential was high, the chlorides might be re-oxidised:

$$TiCl_2 + O_2 \rightarrow TiO_2 + Cl_2 \quad (5)$$

$$2AlCl_3 + 3/2O_2 \rightarrow Al_2O_3 + 3Cl_2 \quad (6)$$

This mechanism implied a self-sustaining corrosion process that required only a very small quantity of chloride phases for continuous reactions. The chlorides played the role of catalysts during the whole reaction.

Meanwhile, the corrosion kinetics of Ti-52Al and Ti-48Al-2Cr followed a parabolic rate law, and showed positive mass changes. Ti-52Al had a microstructure of single γ-phase with relatively high Al content, resulting in an Al-rich scale. The XRD spectra shown in Fig.3 support these mechanisms, as the peaks of α-Al_2O_3 from Ti-52Al were stronger than those from Ti_3Al. Ti-48Al-2Cr also has good hot corrosion resistance, implying that Cr might have a positive influence on the corrosion process. According to Brady *et al.* /17,18/, the substitution of Cr for Ti in sufficient quantities may result in the formation of Laves phase $Ti(Cr,Al)_2$, which exhibits a low oxygen permeability and is capable of forming a protective Al_2O_3 scale. However, the content of Cr in this alloy is small, only 2%, formation of Laves phase would be difficult, other factors, therefore, should play their roles.

EDS was performed on the cross-section shown in Fig. 6, showing that the scale was a mixture of TiO_2 and Al_2O_3. Along the interface between the scale and the substrate of Ti-48Al-2Cr, a thin layer of light contrast could be observed. EDS quantitative analysis showed that this phase has a composition of O = 11.6, Al = 31.7, Ti = 51.3, Cr = 2.8 and N = 2.6, in at.%, very close to the so called "Z-phase", $Ti_{50}Al_{30}O_{20}$, reported in literature /19/. The formation mechanism of Z-phase had been suggested as:

$$\gamma\text{-}Ti_{50}Al_{48} + 2O \rightarrow Z\text{-}Ti_{50}Al_{30}O_{20} + 18Al. \quad (7)$$

The aluminium released in this reaction may diffuse outward to form an Al_2O_3 scale. It was reported that the Z-phase, to a certain degree, could stabilise Al_2O_3, though it was also found that the Z-phase was metastable and eventually decomposed to α_2-$Ti_3Al(O)$ and Al_2O_3 /19/. Thereby, the improvement in hot corrosion resistance may be caused by the formation of the Z-phase.

It was reported that niobium additions could greatly improve the room-temperature mechanical properties of Ti_3Al /20/. Moreover, a 10 at.%Nb could decrease the oxidation rate to a low level although the oxide scale

still consists mainly of TiO_2 with small amount of alumina /21-23/. However, Ti_3Al-11Nb showed the worst hot corrosion and spallation resistance in the present case. This was not expected and is difficult to explain. A possible mechanism is suggested as follows:

It was observed that sulphur penetrated through the oxide scale into the substrate material, and made a thin Ti_8S_3 layer on the interface. Ti_8S_3 does not have good adhesion to the substrate, so neither could the corrosion scale. This allowed the corrosion scale, which mainly consisted of TiO_2 and α-Al_2O_3, to separate more easily from the substrate. The substrate material was now directly exposed to the corrosive salt vapor, resulting in more severe corrosion. XRD and cross-section SEM results support this mechanism, as it could be seen that the flake of corrosion scale mainly contained TiO_2 (Fig. 3), while the spectrum of the remaining specimen after hot corrosion was totally different to that of the flake. It was mainly composed of Ti_8S_3, which can be seen as the thin interface scale between the substrate and Cu-plating in Fig. 7. It could also be seen that the light (marked A) area close to the interface became thinner than inside of the sample, probably because of the outward diffusion of Nb. However, how the diffusion of Nb can affect the formation of Ti_8S_3 is still not clear. More detailed study is needed to fully understand this mechanism.

5. CONCLUSIONS

Six Ti-Al intermetallics, Ti_3Al, Ti-44Al, Ti-48Al, Ti-52Al, Ti-48Al-2Cr and Ti_3Al-11Nb, were exposed to 80 wt%Na_2SO_4 + 20 wt%NaCl vapour containing environments at 800°C up to 200 hrs. Their hot corrosion resistance generally increases with increasing Al content. For instance, Ti-52Al showed better corrosion resistance than Ti-48Al. The latter suffered high corrosion rate and severe oxide scale spallation. This can be explained as the activity of Al in Ti-Al system decreases sharply when %Al decreases from 52% to 48%; and the scale containing higher Al content has better corrosion resistance.

Ti-48Al-2Cr showed the best corrosion resistance among the six alloys. It is believed that its high Al content and Cr addition played a role in forming an oxide scale with relatively good protective ability. Also, the formation of Z-phase, $Ti_{50}Al_{30}O_{20}$, may provide extra corrosion resistance to Ti-48Al-2Cr.

Among the six Ti-Al intermetallics, Ti_3Al-11Nb showed the highest corrosion rate and the worst scale spallation. It is believed that the relatively low Al content might reduce the formation of Al oxides; and the Nb addition might accelerate the formation of sulphide at the interface, playing a detrimental role in the corrosion process.

6. ACKNOWLEDGEMENTS

The authors would like to thank Dr. Quadakkers for providing Ti-48Al-2Cr samples, and the technical staff at the Department and Research Centre for Surface and Materials Science for their assistance.

REFERENCES

1. F.H. Fores, C. Suryanarayana and D. Eliezer, *J. Mater. Sci.*, **27**, 5113 (1992).
2. C.M. Austin and T.J. Kelly, in *Structural Intermetallics*, ed. R. Darolia, J.J. Lewandowski, C.T. Liu, P.L. Martin, D.B. Mirade and M.V. Nathal, TMS, Warrendale, PA, USA (1993) 143.
3. S.C. Huang and E.L. Hall, *Metall Trans.*, **22A**, 427 (1991).
4. J. Stringer, *Mater. Sci. Technol.*, **3**, 483 (1987).
5. R.A. Rapp, *Corrosion*, **42**(10), 568 (1986).
6. Y.W. Kim, *JOM*, **42**, 24 (1989).
7. Y.W. Kim, *JOM*, **47**, 38 (1995).
8. B.D. Craig, *Handbook of Corrosion Data*, ASM International, Materials Park, Ohio, (1989).
9. Z. Li and W. Gao, Corrosion, Oxidation and Mechanical Properties of Titanium, Titanium Alloys and Titanium Composites. An Internal Report, The University of Auckland (2000).
10. Z. Tang, F. Wang and W. Wu, *Mater. Sci. Eng.*, **276**, 70 (2000).
11. Z. Tang, F. Wang and W. Wu, *Intermetallics*, **7**, 1271 (1999).
12. Z. Tang, F. Wang and W. Wu, *Chin. Soc. Corros. Protec.*, **17**, 233 (1997).

13. C. Guan, Z. Tang, F. Wang and W. Wu, *Corros. Sci. Prot. Technol.*, **12**, 134 (2000).
14. J. Takahashi, Y. Kawai and S. Shimada, *J. Europ. Ceram. Soc.*, **18**, 1121 (1998).
15. K. Zhang, Z. Li and W. Gao, in press in *Materials Letters* (2002).
16. Z. Tang, F. Wang and W. Wu, *Oxid. Met.*, **51**, 235 (1999).
17. M.P. Brady, J.L. Smialek, D.L. Humphrey and J. Smith, *Acta Mater*, **45**(6), 2371 (1997).
18. E.H. Copland, B. Gleeson, and D.J. Young, *Acta Mater*, **47**, 2937 (1999).
19. M.P. Brady, J.L. Smialek, J. Smith and D.L. Humphrey, *Acta Mater.*, **45**(6), 2357 (1997).
20. Y. Wu, D.Z. Yang and G.M. Song, *Intermetallics*, **8**, 629 (2000).
21. M. Yoshihara, K. Miura, *Intermetallics*, **3**, 357 (1995).
22. Z.W. Li, W. Gao and Y. He, *Scripta Materialia*, **45**, 1099 (2001).
23. Z. Li, W. Gao, S. Li, D. Zhang and Y. He, *Oxidation of Metals*, **56**, 495 (2001).